Journal of Applied Electrochemistry (2007) 37:129–136
DOI 10.1007/s10800-006-9208-x

Modelling the porous cathode of a SOFC: oxygen reduction mechanism effect

J. DESEURE[1], Y. BULTEL[2,*], L. DESSEMOND[2], E. SIEBERT[2] and P. OZIL[2]
[1]*LEMTA, UMR 7563, 2 Avenue de la Forêt de Haye, BP 160, 54504, Vandoeuvre-les-Nancy, France*
[2]*LEPMI, UMR., CNRS-INPG-UJF 5631 ENSEEG, BP 75, 38402, Saint Martin d'Heres, France*
*(*author for correspondence, tel.: + 33-476-826580, e-mail: Yann.Bultel@lepmi.inpg.fr)*

Received 14 February 2006; accepted in revised form 6 July 2006

Key words: ac impedance, composite cathode, modelling, oxygen reduction, SOFC

Abstract

A composite electrode comprising a porous mixture of solid electrolyte (typically yttria stabilized zirconia, YSZ) and electronically conducting, electrocatalytic material (typically strontium doped lanthanum manganite, LSM) is generally used to improve the cathodic performance of the solid oxide fuel cell (SOFC). The advantage of the composite electrode is that the reaction zone is spread from the electrode/electrolyte interface into the electrode, effectively resulting in a functionally diffuse interface where the charge transfer reaction occurs. The present study proposes a one-dimensional dc and ac model that takes into account mass and charge conservation, transport of species and reaction kinetics. It considers the porous electrode to be a homogeneous medium characterized by a number of parameters, and in particular ionic conductivity and the diffusion coefficient. The influence of kinetic and transport parameters as well as that of the microstructure on the shape of both polarization curves and impedance diagrams is discussed.

List of Symbols

av_{ads}	specific surface area of adsorption (m^{-1})
av_{tpb}	specific electrochemical surface area (m^{-1})
C_{dl}	double-layer capacitance (F m^{-2})
c_O2	oxygen concentration in the gas phase (mol m^{-3})
c_v^{YSZ}	oxygen ion concentration in the electrolyte (mol m^{-3})
D_k	Knudsen diffusion coefficient (m^2 s^{-1})
d_g	spherical particle diameter (m)
d_p	pore diameter (m)
F	Faraday constant (96 485 C mol^{-1})
i	current density (A m^{-2})
k_i	"electrochemical" kinetic constant of the ith reaction (mol^{-1} m^3 s^{-1} or atm^{-1} mol^{-1} m^2 s^{-1})
L	electrode thickness (m)
M_O2	oxygen molecular weight (kg mol^{-1})
R	ideal gas constant (8.31 J K^{-1} mol^{-1})
r_i	reaction rate of the elementary step i (mol m^{-3} s^{-1})
T	temperature (K)
t	time (s)
y	abscissa (m)
Z	electrode impedance (Ω m^2)
Z_f	Faradaic impedance (Ω m^2)
$Re(Z)$	impedance real part (Ω m^2 Pt)
$Im(Z)$	impedance imaginary part (Ω m^2 Pt)

Greek symbol

α	charge transfer coefficient (–)
Γ	maximal concentration of adsorbed species (mol m^{-2})
ε	gas porosity (–)
ε_a	volume fraction of YSZ (–)
ε_{fcc}	porosity of the cubic face centred lattice (–)
η	overpotential (V)
κ	ionic conductivity (S m^{-1})
τ	tortuosity factor (–)
θ	oxygen absorbed coverage rate (–)

1. Introduction

A composite electrode comprising a porous mixture of a solid electrolyte (typically yttria stabilized zirconia, YSZ) and an electronically conducting material (typically strontium doped lanthanum manganite, LSM) is generally used to improve the cathodic performance of solid oxide fuel cells (SOFC). Many studies have demonstrated that composite cathodes exhibit much lower overpotentials than single-phase electrodes by virtue of the parallel paths of ionic and electronic charge carriers [1]. Using a composite cathode enables the

reaction zone to spread from the electrode/electrolyte interface into the electrode and effectively results in a functionally diffuse interface where the charge transfer reaction takes place.

It is generally accepted that the performance of composite cathodes in SOFC is largely governed by interfacial kinetics, mass transport and ohmic drop. Steady-state polarization studies of these electrodes are therefore not sufficient to determine either the limiting processes or the reaction mechanism. Electrochemical impedance spectroscopy (EIS) is used to identify and characterize the various phenomena involved in electrode reaction with a view to optimizing the entire process [2, 3]. However, most studies have focused on the optimization of cathode structure and composition rather than on kinetic mechanisms [4–8].

In an earlier study [9], a theoretical model was proposed for a porous composite cathode. This provided a detailed description of electrode structure and of the processes occurring therein, and considered the activation and mass transport steps. The role of composition, porosity and grain size was first discussed assuming a homogeneous electrode composition. The relative roles of composition and porosity gradients in a porous composite electrode [10] were then theoretically predicted in order to gain a better understanding of the behaviour of a graded electrode and its influence on ionic current flow.

The aim of the present study is to simulate both dc and ac responses under polarization of a composite cathode. In the presence of a constant current, potential and concentration gradients are observed within the composite cathode. In such a case, where a multi-step mechanism is involved, only numerical solutions are available for estimating current distribution and impedance [11]. The theoretical elements of dc and ac models are developed for a composite cathode, taking into account both diffusion and ionic ohmic drop. They are used in a quantitative analysis of impedance spectra in which special attention is paid to characterization of the processes occurring in the gas diffusion electrode during the electrochemical reaction. It should be noted that ionic and electronic percolation thresholds are assumed in this model.

2. Dc and ac model for a composite cathode

2.1. *Oxygen reduction mechanism*

The composite electrode, deposited on dense YSZ and without any composition or porosity gradients, consists of a monodisperse porous mixture of ionic (YSZ) and electronically conducting (M) grains surrounded by gas-filled pores. Oxygen is transported through the porous electrode by diffusion of molecular oxygen in the gas phase. Diffusion of molecular oxygen is considered to be predominantly of the Knudsen type given that the average pore size d_p is fixed at 1 μm [9]. This assumption is consistent with the model of Adler et al. [12]. The flux of oxygen vacancies in YSZ is a function of the electric field while electron transport obeys Ohm's law.

The adsorbed oxygen is formed from oxygen gas according to a dissociative adsorption step that occurs on the pore walls (regardless of particle nature):

$$O_2 + 2s \rightarrow 2O\text{-}s \tag{1}$$

where s stands for an adsorption site and O-s for the adsorbed oxygen.

The adsorbed oxygen is reduced at the three-phase boundary with consumption of an oxygen vacancy $V_0^{\cdot\cdot}$ from YSZ, creation of two holes $h^{\cdot}$ in M and incorporation of an oxygen ion O_0^X into YSZ:

$$O\text{-}s + V_0^{\cdot\cdot} \rightarrow 2h^{\cdot} + O_0^X + s \tag{2}$$

Assuming a Langmuir isotherm, a hypothesis that is consistent for the high temperature range, the rate of chemical dissociative adsorption (1) at the gas/M–YSZ interface depends on the oxygen concentration c_{O2}, (assuming an oxygen partial pressure of 1 atm in the gas channel) and on the relative coverage θ of adsorbates O-s according to:

$$r_{ads} = av_{ads}\Gamma^2\left(k_{ads}c_{O2}(1-\theta)^2 - k_{des}\theta^2\right) \tag{3}$$

where k_{ads} and k_{des} are the adsorption and desorption kinetic constants, av_{ads} the specific adsorption surface area of the electrochemical reaction and Γ is the maximum concentration of adsorbed species ($=10^{-5}$ mol m^{-2}).

The charge transfer rate (2) is given by

$$r_e = av_{tpb}\Gamma\left(k_e \exp\left(-\frac{2\alpha F}{RT}\eta\right)\theta c_v^{YSZ} - k_{-e}\exp\left(\frac{2(1-\alpha)F}{RT}\eta\right)(1-\theta)\right) \tag{4}$$

where η is the electrode overpotential, k_e and k_{-e} are the forward and backward electrochemical kinetic constants, c_v^{YSZ} the oxygen vacancy concentration in the electrolyte (6×10^3 mol m^{-3}), α the symmetry factor and av_{tpb} is the specific electrochemical surface area.

2.2. *Homogeneous model for a composite electrode*

Figure 1(a) is a schematic representation of the composite cathode used for model development, showing the electrode sandwiched between the electronic conductor|gas distributor and the electrolyte pellet. In this study, only the electrochemical behaviour of the composite cathode is modelled; the additional resistances related to current collector/electrode and electrode/electrolyte interfaces are therefore not considered.

The composite cathode is treated as a homogeneous medium characterised by an effective ionic conductivity κ^{eff} dependent on electrode microstructural parameters [9]. The homogeneous model [13] assumes that gas partial pressure, concentration of adsorbed species and overpotential are uniform over the geometrical surface

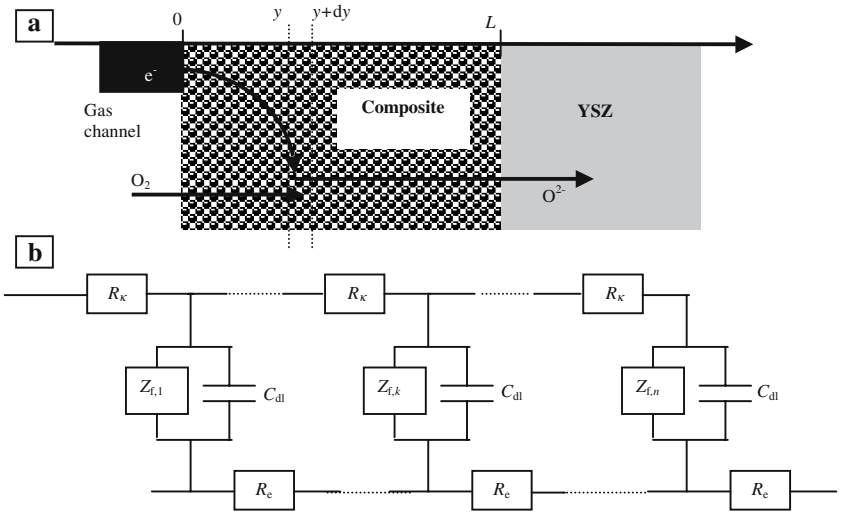

Fig. 1. (a) Schematic representation of a composite cathode and (b) transmission line for an active layer (R_κ: ionic resistance, Z_{fk}: Faradaic impedance, C_{dl}: double-layer capacitance and R_e: electronic resistance).

area of the electrode. Ohmic losses in the electronic conduction phase are ignored, given the appropriate electrical connections, and this phase may therefore be regarded as equipotential. The dc model developed by Deseure et al. [9] is extended to include the dynamic charging processes of the electrical double layer that occur in parallel to the faradaic charge transfer processes (Figure 1(b)).

This one-dimensional model of the composite cathode is then developed by taking into account mass and charge conservation, species transport and reaction kinetics. The continuity equations for the variations in the concentration of gaseous oxygen and covered sites for a porous medium can be classically written as

$$\frac{\partial c_{O2}}{\partial t} - D_k \frac{\partial^2 c_{O2}}{\partial y^2} + r_{ads} = 0 \tag{5}$$

$$av_{ads}\Gamma \frac{\partial \theta}{\partial t} = 2r_{ads} - r_e \tag{6}$$

The continuity equation related to the transformation of ionic species into electronic current, via faradaic processes and double-layer charging, is given by

$$av_{tpb}C_{dl}\frac{\partial |\eta|}{\partial t} - \kappa^{eff}\frac{\partial^2 |\eta|}{\partial y^2} + 2Fr_e = 0 \tag{7}$$

Solving this set of equations provides the concentration and overpotential distributions and thus both current density and impedance [11]. In the case of a composite cathode, the gas phase diffusion of oxygen is predominantly of the Knudsen type [9] for pore sizes of less than 10 μm and the diffusion coefficient D_k may be defined as a function of pore diameter, d_p [14]:

$$D_k = d_p \frac{\varepsilon}{3\tau}\sqrt{\frac{8RT}{\pi M_{O_2}}} \tag{8}$$

while the composite electrode (porous medium) should be described as a stacking of spherical-shape grains [9, 14] with a specific adsorption surface area expressed in relation to the diameter as

$$av_{ads} = \frac{6}{d_g}(1-\varepsilon) \tag{9}$$

where d_g is the grain diameter and ε is the porosity of the porous electrode. The specific electrochemical surface area can be also corrected from the porosity according to [9] as follows:

$$av_{tpb} = av_{tpb\_0}\left(1 - \frac{\varepsilon - \varepsilon_{fcc}}{1-\varepsilon_{fcc}}\right)\frac{{d_{g_0}}^3}{d_g^3} \tag{10}$$

In this expression, when porosity is lower than the porosity of a face-centred cubic lattice ($\varepsilon_{fcc} = 1-(\pi/3\sqrt{2}) \approx 0.26$), the electrochemical specific area is fixed at av_{tpb}_0, and the arbitrary value of electrochemical specific area ($av_{tpb}\_0 = 10^6\ m^{-1}$) for the initial grain diameter ($d_g0 = 1\ \mu m$).

The expression of pore diameter [9] can be expressed as follows:

$$d_p = \frac{4\varepsilon}{av_{ads}} \tag{11}$$

Finally, the effective ionic conductivity (κ^{eff}) depends on electrode geometrical characteristics such as porosity, tortuosity and the volume fraction of electrolyte ε_a in the granular mixture:

$$\kappa^{eff} = \varepsilon_a \frac{1-\varepsilon}{\tau}\kappa \tag{12}$$

3. Results and discussion

The following subsection discusses the influences of transport phenomena and the oxygen reduction mechanism on the shape of both polarization curves and impedance diagrams. In composite electrodes, activation and diffusion limitations, as well as an ohmic drop

contribution, can occur simultaneously [15]. Accordingly, some limiting cases are also studied to gather information on each separate effect. Mass and charge transport phenomena are investigated assuming that the adsorption step remains at equilibrium ($r_{ads} = 0$), while the oxygen reduction mechanism is studied by considering both chemical and electrochemical processes.

Table 1 lists the standard values of the parameters required to perform numerical simulations. The effects of microstructure parameters will be examined at the end of this discussion. Kinetic constants were chosen in order to obtain cathodic current densities similar to those recorded under SOFC working conditions. The influence of some of these parameters will be discussed in the following sections and compared with the standard case.

3.1. *Mass transport limitations: diffusion and migration*

The effect of mass and charge transport within the porous electrode cannot be easily demonstrated in the absence of a limiting current. Therefore it is much more difficult to distinguish the effects of gas diffusion and ionic ohmic drop on the electrode performances from those of the geometric parameters. Exponential activation behaviour was observed for kinetic control limited by either electrochemical reaction or mass and charge transport ($r_{ads} = 0$) [9]. For very slow electrochemical reactions, oxygen reduction is under kinetic control and thus diffusion and ohmic drop resistances are negligible compared with charge transfer resistance, whereas related resistances are no longer negligible.

When diffusion in the active layer controls process kinetics, it is well known that no limiting current behaviour occurs and that a doubling of the effective Tafel slope is observed on steady-state polarization curves [16]. Figure 2 shows impedance diagrams simulated for various values of D_k ranging from 4×10^{-5} to 10^{-8} m^2 s^{-1}. This latter parameter affects the shapes of concentration profiles and complex plane plots. The model provides insights into how gaseous diffusion limitation acts on both dc and ac responses. Under kinetic control (i.e. for a high diffusion coefficient or low current density), diffusion is fast enough to supply the reacting species to the triple phase boundary and the concentration profile remains close to a constant value in the porous cathode. In this simplest case, the complex plane plot is reduced to a semicircle, which corresponds, as expected, to the only charge transfer resistance that is in parallel with the double-layer capacitance (Figure 2). With increasing diffusion limitations, a steeper concentration gradient is predicted and an additional capacitive loop can be distinguished on the low frequency side, in agreement with experimental impedance diagrams observed for low oxygen partial pressures and/or high temperatures [6, 17]. Nevertheless, a well-defined separation of the high frequency (charge transfer) and low frequency (diffusion) arcs can clearly be observed for a very small double-layer capacitance [16]. Decreasing this capacitance results in a shift in the apex frequency of the charge transfer arc towards higher values, and the diffusion impedance can thus be represented as a nearly perfect semicircle [18, 19]. This means that the existence

Table 1. Standard physical and chemical parameters used for simulations

Parameters	Parameters		
Electrode thickness (L)	50 μm	Adsorption kinetic constant (k_{ads})	10^{-5} m^4 mol^{-2} s^{-1}
Electrode porosity (ε)	30%	Desorption kinetic constant (k_{des})	10^{-2} mol^{-1} m^2 s^{-1}
Specific surface area of adsorption (av_{ads})	4.2×10^6 m^{-1}	Forward kinetic constant (k_e)	0.12 mol^{-1} m^3 s^{-1}
Specific electrochemical surface area (av_{tpb})	10^6 m^{-1}	Symmetry factor (α)	0.5
Diffusion coefficient (D_k)	10^{-8} to 4×10^{-5} m^2 s^{-1}	Temperature (T)	1073 K
Ionic conductivity (κ)	2 to 200 S m^{-1}	Pressure (P)	10^5 Pa
Double-layer capacitance (C_{dl})	0.32 F m^{-2}	Volume fraction of the electrolyte (ε_a)	50%

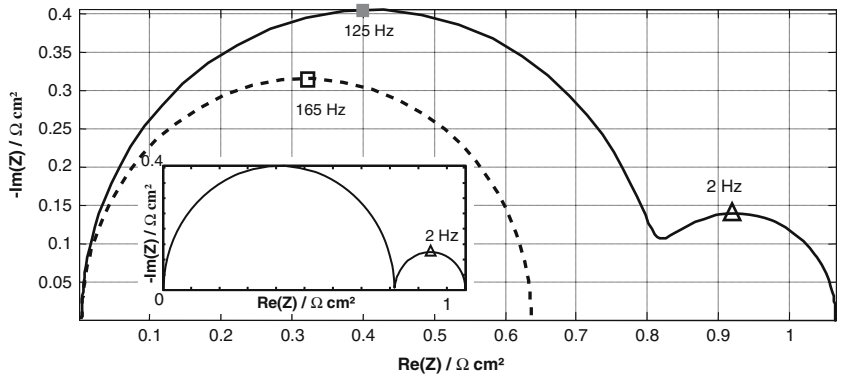

Fig. 2. Simulated impedance diagrams of a composite cathode ($|\eta| = 400$ mV): influence of the diffusion coefficient (- - -: $D = 4 \times 10^{-5}$ m^2 s^{-1}; —: $D = 10^{-8}$ m^2 s^{-1} and $C_{dl} = 10^{-3}$ F m^{-2}).

of a low frequency loop is directly related to the oxygen concentration gradient in the composite cathode. Under the operating conditions of a SOFC (high oxygen partial pressure, temperature below 900 °C), O_2 diffusivity is sufficiently high (typically $D_k > 10^{-8}$ m^2 s^{-1}) [17]. Moreover, since the magnitude of the double-layer capacitance can be considered as a few 10s of mF m^{-2} [20], one can expect that gaseous diffusion impedance would not be shown, even under cathodic polarization [21].

Figures 3 and 4 show potential distribution in a composite cathode and the corresponding impedance diagrams for various κ values ranging from 2 to 200 S m^{-1}. As shown in Figure 4, a 45° straight line is obtained in the high-frequency range when ionic drop resistance is increased. This behaviour can be attributed to double-layer charging and ionic transport within the composite electrode, processes which dominate the overall electrode response. The occurrence of a high frequency contribution in the impedance response of a LSM–YSZ composite electrode has already been ascribed to ionic transport through the YSZ [6]. The equivalent circuit signal is a RC-transmission-line as shown in Figure 1(b). However, ionic ohmic drop effects can be ignored at low frequencies. At this stage, it is worth mentioning that diffusion limitation is negligible for a thin composite cathode whereas a thicker composite cathode can induce diffusion limitation as well as an ionic ohmic drop, depending on the experimental conditions. The magnitude of YSZ conductivity is expected to be a few S m^{-1} in SOFC operating conditions. The high frequency line related to ionic transport limitation may thus be anticipated.

3.2. *Effect of the kinetic mechanism*

Let us now consider the entire two-step mechanism of oxygen reduction (Eqs. 1 and 2) involving the diffusion of O_2 species in the gas phase and the adsorption of intermediate species O-s on the material surface within the porous electrode. When the electrode reaction rate is controlled by both chemical and electrochemical steps, the polarization curve exhibits Tafel-like behaviour (activation polarization) at low overpotential and a limiting current density related to oxygen adsorption at high cathodic overpotential [9].

The impedance diagrams are in this case composed of either one or two semicircles, depending on adsorption kinetic constants and electrode overpotential (Figure 5). For a very fast adsorption step, only one capacitive arc

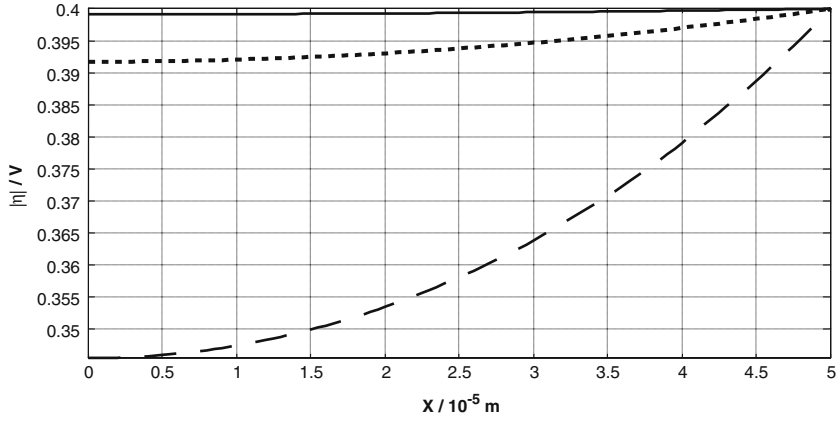

Fig. 3. Steady-state overpotential profile in a composite cathode region (|η| = 400 mV): influence of ionic conductivity (—: κ = 200 S m^{-1}; ···: κ = 20 S m^{-1}; - - -: κ = 2 S m^{-1}).

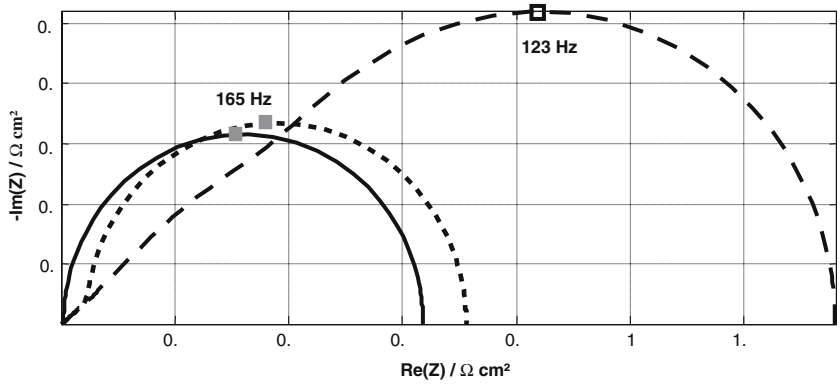

Fig. 4. Simulated impedance diagrams of composite cathode (|η| = 400 mV): influence of ionic conductivity (—: κ = 200 S m^{-1}; ···: κ = 20 S m^{-1}; - - -: κ = 2 S m^{-1}).

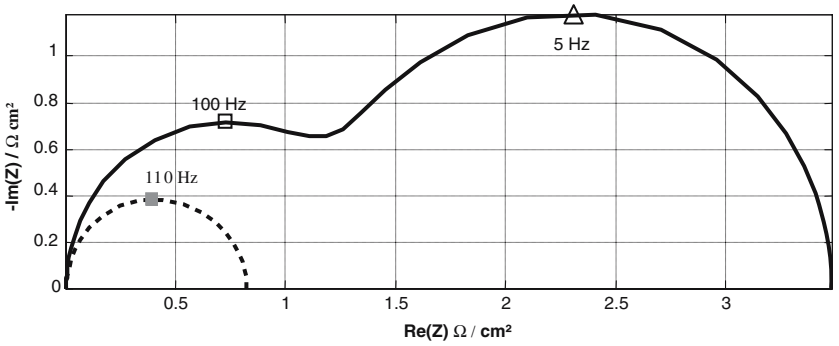

Fig. 5. Simulated impedance diagrams of a composite cathode ($|\eta|$ = 400 mV): influence of the adsorption kinetic rate (- - -: $k_{ads} = 10^{-5}$ m^4 mol^{-2} s^{-1}; —: $k_{ads} = 10^{-6}$ m^4 mol^{-2} s^{-1}).

is observed, corresponding to the charge transfer resistance connected in parallel with the double layer. When the adsorption kinetic effect is increased (i.e. for a slow adsorption step), an additional low frequency semicircle appears, which is classically attributed to the concentration impedance of the intermediate adsorbed species O-s [2].

3.3. *Effect of microstructure*

As shown above, pore diameter (Eq. 11), specific adsorption surface area (Eq. 9) and effective mass transport coefficients (Eqs. 8–12) can be calculated from composite electrode composition (ε_a), porosity (ε) and grain diameter (d_g). Kinetic constants were chosen in order to obtain the same cathodic current densities as those observed in the previous sections. Then, ε and d_g were varied in the simulation. As demonstrated by dc simulations [9], decreasing the grain diameter improves electrode performance for increases in both the specific electrochemical surface area and the adsorption surface. This result is in agreement with the findings of Zhao et al. [22] for a LSM–YSZ composite cathode. However, the effect of mass and charge transport within the porous electrode cannot be easily demonstrated since no limiting current behaviour is observed in the porous electrode. Thus calculations may highlight the occurrence of limiting steps that occur inside the composite electrode.

Figure 6 shows simulated impedance diagrams for different porosity values (1.5–25.5%). Grain diameter d_g was kept equal to 1 μm and effective ionic conductivity was fixed at 2 S m^{-1}. These diagrams emphasize the competition between mass and charge transport. Increasing porosity increases mass transport and causes the low frequency arc to vanish, while polarization resistance decreases. When ionic ohmic drop becomes limiting, resistance polarization further increases with porosity.

This result shows that electrode granulometry is a key parameter, as has been suggested in experiments [23]. Moreover, as proved by dc simulation [9], the origin of the limiting process depends on d_g: for the lowest grain diameters, the dissociative adsorption step dominates the electrode process. This behaviour is in agreement with the theoretical equations expressing adsorption and electrochemical specific areas as a function of grain diameter (Eqs. 9–11).

Simulated impedance diagrams for various d_g values are shown in Figure 7. For a fixed porosity, regardless of the double-layer capacitance, polarization resistance decreases with grain size. As for mass transport limitations (Figure 2), at low C_{dl} values, two contributions can be distinguished: a high frequency electrochemical step and a low frequency adsorption step. The relative magnitude of these contributions thus changes with grain size. Following the discussion on the kinetics

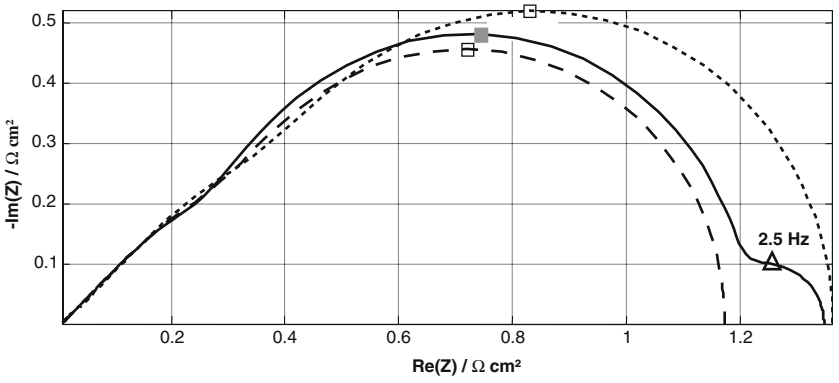

Fig. 6. Simulated impedance diagrams of a composite cathode ($|\eta|$ = 400 mV; κ = 2 S m^{-1} and d_g = 1 μm): influence of porosity (—: ε = 0.7%;···: ε = 10%; - - -: ε = 30%) ■: apex frequency value = 107 Hz; □ apex frequency value = 123 Hz.

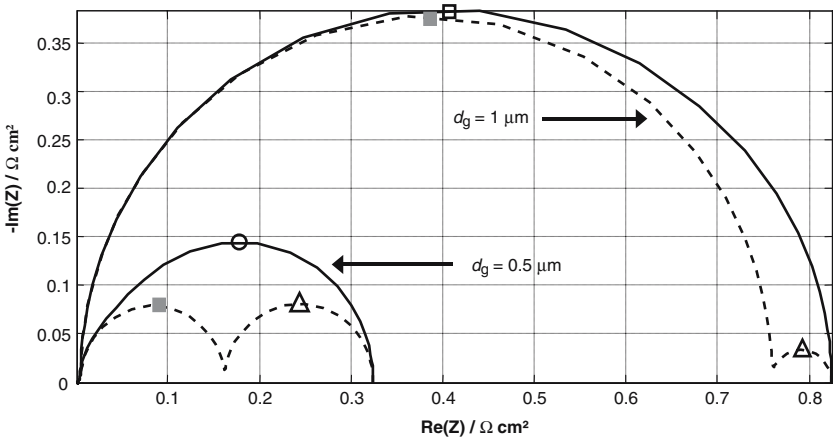

Fig. 7. Simulated impedance diagrams of a composite cathode ($|\eta|$ = 400 mV; κ = 200 S m^{-1}): influence of grain diameter $1 \leq d_g \leq 0.5$ μm (—: C_{dl} = 0.32 F m^{-2};···: $C_{dl} = 10^{-3}$ F m^{-2}) ■: apex frequency value = 40 kHz; □: apex frequency value = 115 Hz; ○: apex frequency value = 22 Hz; △: apex frequency value = 30 Hz.

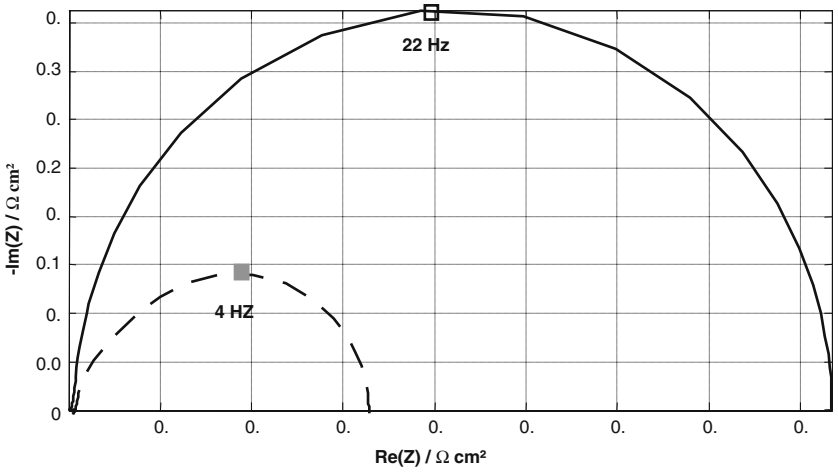

Fig. 8. Simulated impedance diagrams of a composite cathode ($|\eta|$ = 400 mV; κ = 200 S m^{-1}): influence of grain diameter (- - -: d_g = 0.5 μm; —: d_g = 0.33 μm).

(Section 3.2), the electrochemical step becomes faster than the adsorption step when grain size becomes smaller, a result that was also confirmed by Deseure et al. [9]. The charge balance equation (Eq. 7) shows that the effective double-layer capacitance is proportional to the specific electrochemical surface area. Thus it is impossible to distinguish between the effects of charge transfer and the adsorption step in the oxygen reduction process.

Figure 8 shows that polarization resistance increases with further decreases in grain size below 0.5 μm. This phenomenon originates in the restricted mass transport due to decreasing pore diameter. It was also difficult to separate mass transport from charge transfer, making it impossible to distinguish individual contributions. Moreover, by taking into account the ionic ohmic drop (Figure 6), the impedance response of the charge transport limitation is almost identical to that of a classical diffusion system (a 45° straight line).

Finally, EIS under polarization is not sufficiently accurate for the elementary steps in the oxygen reduction process to be observed separately.

4. Conclusion

A one-dimensional homogeneous model was developed to obtain insights into the performance characteristics of a composite porous SOFC cathode, taking into account the oxygen adsorption, charge transfer as well as mass and charge transport processes (ionic migration, Knudsen-type gas phase diffusion). Applying this model shows that, even if diffusion and migration processes play a crucial role, the overall reaction is never completely governed by these processes. Diffusional limitation leads to a low frequency semicircle and ionic ohmic drop to a high frequency straight line in a complex plane plot. Thus, the contribution of gaseous diffusion remains less than that of the ionic ohmic drop process. Even when the ionic ohmic drop limitation is difficult to detect on the polarization curves, a useful indicator on the complex plane plot is the straight-line feature in the high frequency region. The impedance diagrams are then composed of either a single capacitive arc or two capacitive arcs, depending on the adsorption kinetic constants and the electrode overpotential.

References

1. J.H. Choi, J.H. Jang and S.M. Oh, *Electrochim. Acta* **46** (2001) 867.
2. E.P. Murray and S.A. Barnett, *Solid State Ionics* **143** (2001) 265.
3. S.P. Jiang, J.G. Love and Y. Ramprakash, *J. Power Sources* **110** (2002) 201.
4. V. Dusastre and J.A. Kilner, *Solid State Ionics* **126** (1999) 163.
5. A.V. Virkar, J. Chen, C.W. Tanner and J.W. Kim, *Solid State Ionics* **131** (2000) 189.
6. M.J. Jorgensen, S. Primdhal, C. Bagger and M. Mogensen, *Solid State Ionics* **139** (2001) 1.
7. R.E. Williford and P. Singh, *J. Power Sources* **128** (2004) 45.
8. W.G. Wang and M. Mogensen, *Solid State Ionics* **176** (2005) 457.
9. J. Deseure, Y. Bultel, L. Dessemond and E. Siebert, *Electrochim. Acta* **50** (2005) 2037.
10. J. Deseure, L. Dessemond, Y. Bultel and E. Siebert, *J. Eur. Ceram. Soc.* **25** (2005) 2676.
11. Y. Bultel, L. Geniès, O. Antoine, P. Ozil and R. Durand, *J. Electroanal. Chem.* **527** (2002) 143.
12. S.B. Adler, J.A. Lane and B.C.H. Steele, *J. Electrochem. Soc.* **143** (1996) 3554.
13. S. Srinivasan, H.D. Hurwitz and J. O'M Bockris, *J. Chem.Phys.* **46** (1967) 3108.
14. J.W. Veldsink, R.M.J. van Damme, G.F. Versteeg and W.P.M. van Swaaij, *Chem. Eng. J.* **57** (1995) 115.
15. Y. Jiang, S. Wang, Y. Zhang, J. Yan and W. Li, *Solid State Ionics* **110** (1998) 111.
16. M. Keddam, C. Rakotomavo and H. Takenouti, *J. Appl. Electrochem.* **14** (1984) 437.
17. K. Huang, *J. Electrochem. Soc.* **151** (2004) H117.
18. A. Lasia, *J. Electroanal. Chem.* **500** (2001) 30.
19. S. Devan, V.R. Subramanian and R.E. White, *J. Electrochem. Soc.* **151** (2004) A905.
20. S.P. Jiang, J.P. Zhang and K. Foger, *J. Electrochem. Soc.* **147** (2000) 3195.
21. H. Orui, K. Watanabe and M. Arakawa, *J. Power Sources* **112** (2002) 90.
22. F. Zhao, Y. Jiang, G.Y. Lin and A.V Virkar, *Electrochem. Soc. Proc.* **16** (2001) 501.
23. S. Wang, Y. Jiang, Y. Zhang, J. Yan and Li W., *Solid State Ionics* **113–115** (1998) 291.